



PERGAMON

International Journal of Solids and Structures 40 (2003) 4125–4133

INTERNATIONAL JOURNAL OF
SOLIDS and
STRUCTURES

www.elsevier.com/locate/ijsolstr

Short communication

Further assessment of a generalized plate model: stress analysis of angle-ply laminates

Shulong Liu ^{a,*}, Kostas P. Soldatos ^b

^a School of Mechanical, Material, Manufacturing Engineering and Management, University of Nottingham, Pope-A20, Nottingham NG7 2RD, UK

^b Theoretical Mechanics Division, University of Nottingham, Pope-B8, Nottingham NG7 2RD, UK

Received 20 February 2003

Abstract

This study is a continuation of the investigation presented in reference (International Journal of Mechanical Sciences 44 (2002) 287) and deals with an assessment of the stress analysis performance of the generalised shear deformable theory presented in (Acta Mechanica 123 (1997c) 163) when dealing with angle-ply laminated beams. One of the main conclusions is that the existing elasticity solutions for simply supported laminates cannot anymore be considered as safe means in checking and testing the effectiveness of other, conventional shear deformable theories, at least as far as angle-ply laminates are concerned.

© 2003 Published by Elsevier Science Ltd.

Keywords: Plate; Stress; Laminates

1. Introduction

It is well known that conventional beam and plate theories yield poor results when dealing with stress analysis predictions in highly reinforced laminated components. A predictor–corrector method that can improve the accuracy of such stress analysis studies has appeared and applied in (Jones, 1975; Sun et al., 1975; Reddy, 1984; DiSciuva, 1986; Noor and Burton, 1990; Savithri and Varadan, 1990; Heuer, 1992; Noor and Malik, 1999; Jane and Hong, 2000). Soldatos and Liu (2001) employed the afore-mentioned predictor–corrector method in connection with the general transverse shear and normal deformable theory (Soldatos and Watson, 1997a,b) and, for a single-layered clamped–clamped beam, they compared displacement and stress results obtained at particular points of the beam span with corresponding exact elasticity predictions (Vel and Batra, 2000). Most recently, Liu and Soldatos (2002) extended this predictor–corrector assessment in connection with cross-ply laminated beams, making however also use of the generalised shear deformable theory (Soldatos and Watson, 1997c).

*Corresponding author. Tel.: +44-115-9514119; fax: +44-115-9514000.

E-mail address: epzsl@nottingham.ac.uk (S. Liu).

This study is a continuation of the investigation presented in (Liu and Soldatos, 2002) and deals with an assessment of the stress analysis performance of the generalised shear deformable theory (G5DOFT) (Soldatos and Watson, 1997c) when dealing with angle-ply laminated beams. Having already been found considerably inaccurate, even when dealing with cross-ply laminates (Liu and Soldatos, 2002), conventional shear deformable theories are not included in the present, further G5DOFT assessment, which based on comparisons of the transverse shear stress distributions obtained by means of the two phases of the aforementioned predictor–corrector method. Relevant equations, mathematical formulas and specific nomenclature details are not included for the sake of brevity. These are detailed in (Liu, 2001) and follow patterns similar to those appearing in previous relevant publications.

2. Presentation of results and further assessment

In the applications to follow, the orthotropic material used in each layer has the following elastic properties:

$$E_L/E_T = 25, \quad G_{LT}/E_T = 0.5, \quad G_{TT}/E_T = 0.2, \quad v_{LT} = v_{TT} = 0.25, \quad (1)$$

except of cases dealing with varying stiffness ratio, E_L/E_T . The lateral beam loading, applied on its top lateral plane, is assumed in the single Fourier-harmonic form:

$$q(x) = q_m \sin(p_m x), \quad p_m = m\pi/L, \quad m = 1, 2, \dots \quad (2)$$

where x is the axial co-ordinate parameter and L is the beam thickness. The beam thickness, h , is mainly determined by the ratio $L/h = 10$ except of cases dealing with varying aspect ratio. This ratio ($L/h = 10$) characterises a moderately thick plate, and in conjunction with the high value of the stiffness ratio E_L/E_T , is considered to be an adequate test of the reliability of both the theoretical model and the method. Some cases of thin and thick, stiff and soft, small and large angle-ply laminates have been examined in order to identify the limitations of the general five-degree-of-freedom beam theory tested. All the numerical results shown in what follows are presented by means of the following non-dimensional parameters:

$$\bar{\tau}_{xz} = \tau_{xz} h / q_m L, \quad \bar{\sigma}_z = \sigma_z / q_m. \quad (3)$$

For simply supported angle-ply laminated beams, the accuracy of the G5DOFT predictions have already been verified in (Shu and Soldatos, 2000) by means of successful numerical comparisons performed with corresponding results based on the existing exact elasticity solutions (Pagano, 1970; Ren, 1986). Accordingly, for either thin or moderately thick plates, the predictor phase of the present approach has shown an excellent performance. Moreover, the predictor phase performs very reliably even for thick SS laminates ($h/L = 0.25$), despite the limitations of G5DOFT. It is denoted in this connection that the shear stress τ_{xz} obtained in the predictor phase satisfies the zero shear stress lateral surface conditions, as well as the interfaces continuity conditions. Being, however, a shear deformable theory only, G5DOFT cannot give σ_z predictions in the predictor phase, which can only be obtained through the corrector phase application. In the corrector phase, shear stress predictions of simply supported beams are always almost identical to their predictor phase counterparts. Hence, given the high accuracy of G5DOFT predictions, corrections of the transverse shear and normal stresses for simply supported beams will not be presented in this Note. Instead, all transverse shear and transverse normal stress results shown are for beams having one end clamped and the other clamped or free (CC and CF beams). These results are for three-layered laminates with thickness ratios of $h_1/h_2/h_3/h = 0.3/0.4/0.3/1.0$ and fibres direction angles at $\alpha_1 = -\alpha$, $\alpha_2 = \alpha$ and $\alpha_3 = -\alpha$.

Table 1 presents numerical values of normalised transverse stresses at selected points that are evenly distributed through the length and thickness of a three-layered CC beam ($\alpha = 30^\circ$). Due to the symmetries

Table 1

Transverse shear and normal stress predictions for three-layered CC beam ($h/L = 0.1$, $\alpha = 30^\circ$)

z/h	$x/L = 0.0$	0.1	0.2	0.3	0.4	0.5
$\bar{\tau}_{xz}$ predictor						
0.5	0	0	0	0	0	0
0.4	0	-0.1534	-0.1408	-0.1042	-0.0551	0
0.3	0	-0.2621	-0.2406	-0.1780	-0.0941	0
0.2	0	-0.3300	-0.3028	-0.2240	-0.1185	0
0.2	0	-0.3800	-0.3206	-0.2298	-0.1202	0
0.1	0	-0.4404	-0.3762	-0.2710	-0.1420	0
0	0	-0.4603	-0.3946	-0.2846	-0.1492	0
$\bar{\tau}_{xz}$ corrector						
0.5	0	0	0	0	0	0
0.4	-1.1370	-0.1998	-0.1468	-0.1059	-0.0556	0
0.3	-0.9642	-0.2949	-0.2433	-0.1786	-0.0943	0
0.2	0.0624	-0.3077	-0.2955	-0.2216	-0.1178	0
0.2	0.0624	-0.3077	-0.2955	-0.2216	-0.1178	0
0.1	0.4131	-0.4350	-0.3782	-0.2717	-0.1422	0
0	0.5576	-0.4760	-0.4053	-0.2882	-0.1503	0
$\bar{\sigma}_z$ corrector						
0.5	0.0000	-0.3090	-0.5878	-0.8090	-0.9511	-1.0000
0.4	2.1412	-0.2362	-0.5675	-0.7846	-0.9227	-0.9702
0.3	5.3610	-0.1272	-0.5215	-0.7224	-0.8490	-0.8926
0.2	6.1687	-0.1041	-0.4681	-0.6373	-0.7457	-0.7834
0.2	6.1687	-0.1041	-0.4681	-0.6373	-0.7457	-0.7834
0.1	3.8279	-0.1369	-0.3942	-0.5300	-0.6188	-0.6498
0	0.0000	-0.1545	-0.2939	-0.4045	-0.4755	-0.5000
-0.1	-3.8279	-0.1721	-0.1936	-0.2790	-0.3323	-0.3502
-0.2	-6.1687	-0.2049	-0.1196	-0.1717	-0.2053	-0.2166
-0.2	-6.1687	-0.2049	-0.1196	-0.1717	-0.2053	-0.2166
-0.3	-5.3610	-0.1818	-0.0663	-0.0867	-0.1020	-0.1074
-0.4	-2.1412	-0.0728	-0.0202	-0.0244	-0.0284	-0.0298
-0.5	0	0	0	0	0	0

of the problem, both the shear $\bar{\tau}_{xz}$ and the transverse normal stress $\bar{\sigma}_z$ have identical through-thickness distributions at x/L and $1 - x/L$. Moreover, due to the fact that, like all shear deformable beam theories, G5DOFT ignores the effects of transverse normal deformation, the through-thickness transverse shear stress predictions, $\bar{\tau}_{xz}$, are symmetric with respect to the beam middle axis. Hence, numerical results for $\bar{\tau}_{xz}$ are only presented for the left and top quarter whereas numerical results for $\bar{\sigma}_z$ are only presented for the left half of the CC beam. Nevertheless, detailed through-thickness distributions of shear and transverse normal stresses obtained via the corrector phase of the present approach are graphically shown in Figs. 1 and 2, respectively.

It is observed that both predictor and corrector phases yield zero shear stresses on the middle cross-section and satisfy the zero shear traction conditions on the lateral surfaces of the beam. Whereas the predictor phase yields discontinuity of $\bar{\tau}_{xz}$ at the interfaces, the interface continuity of $\bar{\tau}_{xz}$ is restored in the corrector phase. As required, $\bar{\sigma}_z$ distributions are continuous at the material interfaces and satisfy the normal stress conditions specified on the beam lateral boundaries. Transverse shear stresses obtained via the predictor and corrector phases have similar distributions in corresponding sections except at the clamped ends. It is observed that the percentage difference of shear stress predictions at the $z = 0$, $x = 0.1L$, where the maximum shear stress occurs, is about 3%. This observation shows that as far as shear stresses

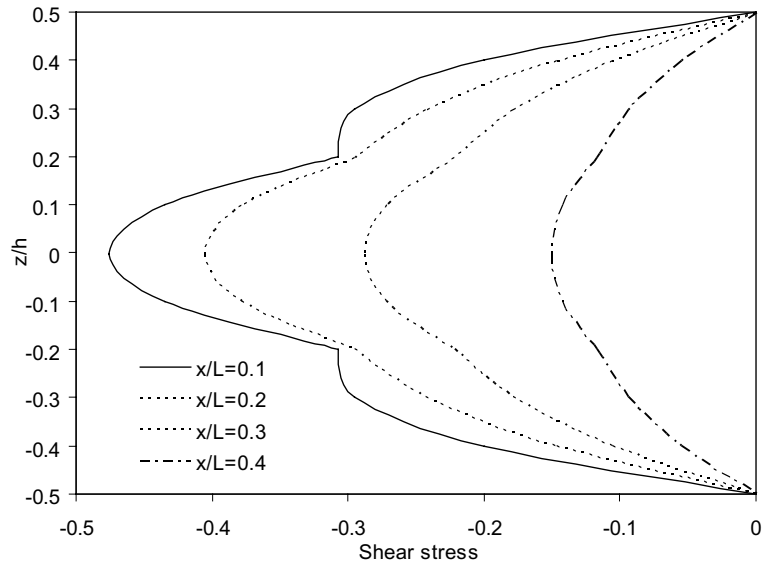


Fig. 1. Normalized shear stress distribution, $\bar{\tau}_{xz}$, in a CC beam (corrector phase).

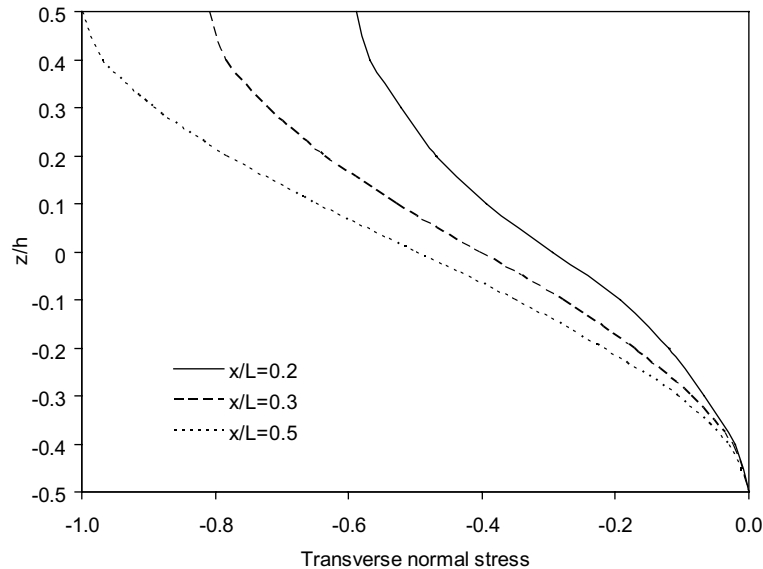


Fig. 2. Normalized transverse normal stress distribution, $\bar{\sigma}_z$, in a CC beam (corrector phase).

are concerned G5DOFT predictions are again very accurate. Here, the transverse shear stress τ_{xz} percentage difference between predictor and corrector phase results is defined as follows:

$$\left| \frac{\tau_{xz}^{(P)} - \tau_{xz}^{(C)}}{\tau_{xz}^{(P)}} \right| \times 100, \quad (4)$$

where $\tau_{xz}^{(P)}$ and $\tau_{xz}^{(C)}$ represent shear stress in predictor phase and corrector phase, respectively.

Table 2

Transverse shear and normal stress predictions for three-layered CF beam ($h/L = 0.1$, $\alpha = 30^\circ$)

z/h	$x/L = 0.0$	0.2	0.4	0.6	0.8	1.0
$\bar{\tau}_{xz}$ predictor						
0.5	0	0	0	0	0	0
0.4	0	-0.3200	-0.2387	-0.1285	-0.0387	-0.0044
0.3	0	-0.5465	-0.4076	-0.2194	-0.0660	-0.0074
0.2	0	-0.6880	-0.5129	-0.2761	-0.0831	-0.0093
0.2	0	-0.7131	-0.5050	-0.2645	-0.0712	0.0026
0.1	0	-0.8396	-0.5995	-0.3155	-0.0866	0.0008
0	0	-0.8812	-0.6306	-0.3322	-0.0916	0.0002
$\bar{\tau}_{xz}$ corrector						
0.5	0	0	0	0	0	0
0.4	-2.2740	-0.3201	-0.2276	-0.1164	-0.0265	0.0078
0.3	-1.9284	-0.5434	-0.3992	-0.2106	-0.0572	0.0014
0.2	0.1247	-0.6781	-0.5167	-0.2813	-0.0885	-0.0147
0.2	0.1247	-0.6781	-0.5167	-0.2813	-0.0885	-0.0147
0.1	0.8262	-0.8453	-0.6017	-0.3172	-0.0883	-0.0009
0	1.1151	-0.9005	-0.6299	-0.3293	-0.0885	0.0034
$\bar{\sigma}_z$ corrector						
0.5	0.0000	-0.5878	-0.9511	-0.9511	-0.5878	0
0.4	4.2997	-0.5646	-0.9226	-0.9228	-0.5703	0
0.3	10.7629	-0.5184	-0.8491	-0.8489	-0.5246	0
0.2	12.3765	-0.4774	-0.7471	-0.7445	-0.4599	0
0.2	12.3765	-0.4774	-0.7471	-0.7445	-0.4599	0
0.1	7.6748	-0.4084	-0.6205	-0.6173	-0.3813	0
0	0.0000	-0.2939	-0.4755	-0.4755	-0.2939	0
-0.1	-7.6748	-0.1794	-0.3306	-0.3338	-0.2065	0
-0.2	-12.3765	-0.1104	-0.2039	-0.2066	-0.1278	0
-0.2	-12.3765	-0.1104	-0.2039	-0.2066	-0.1278	0
-0.3	-10.7629	-0.0694	-0.1019	-0.1022	-0.0631	0
-0.4	-4.2997	-0.0231	-0.0285	-0.0283	-0.0175	0
-0.5	0	0	0	0	0	0

Table 2 presents similarly numerical values of normalised transverse shear and normal stress distributions for a three-layered CF beam ($\alpha = 30^\circ$). The shear stress, $\bar{\tau}_{xz}$, distributions occur again in symmetric form with respect to the beam middle axis and, hence, the corresponding numerical results are only presented for the top half of the beam. Associated complete through-thickness distributions of transverse shear and normal stresses obtained through the corrector phase of the present approach are also shown graphically in Figs. 3 and 4, respectively. Both predictor and corrector phases yield non-zero but very small (essentially negligible) shear stress values at the free end. The predictor phase yields discontinuous shear stress distributions at the interfaces and negligible non-zero values on the lateral boundaries. Both the transverse shear and the normal stress distributions satisfy however interlaminar continuity and lateral boundary conditions in the corrector phases. The transverse shear stress distributions obtained through the predictor and corrector phases have again similar forms in corresponding cross-sections, except at the ends. The percentage error at the $z = 0$, $x = 0.1L$, where the maximum shear stress occur, is less than 3%, thus showing again that the shear stress predictions of G5DOFT are already very accurate.

Table 3 presents the variation of shear stress values for varying angles, span and stiffness ratios of a CC beam. It is noted that, at the points $z = 0$ of the selected cross-sections, transverse shear stresses are close to their maximum values (Table 1). The point $(0.25L, 0)$ is selected to investigate variations of the shear stress $\bar{\tau}_{xz}$ with varying angles, span and stiffness ratios. For the purpose of observing the influence of the interface

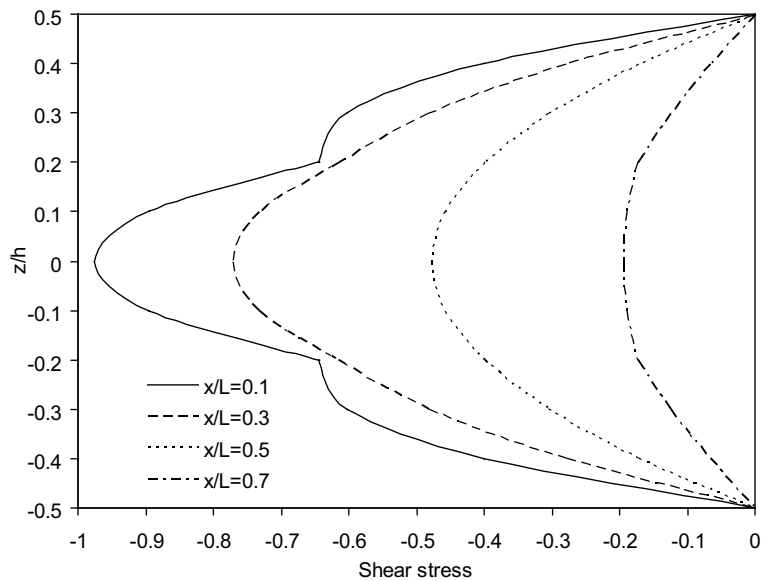


Fig. 3. Normalized shear stress distribution, $\bar{\tau}_{xz}$, in a CF beam (corrector phase).

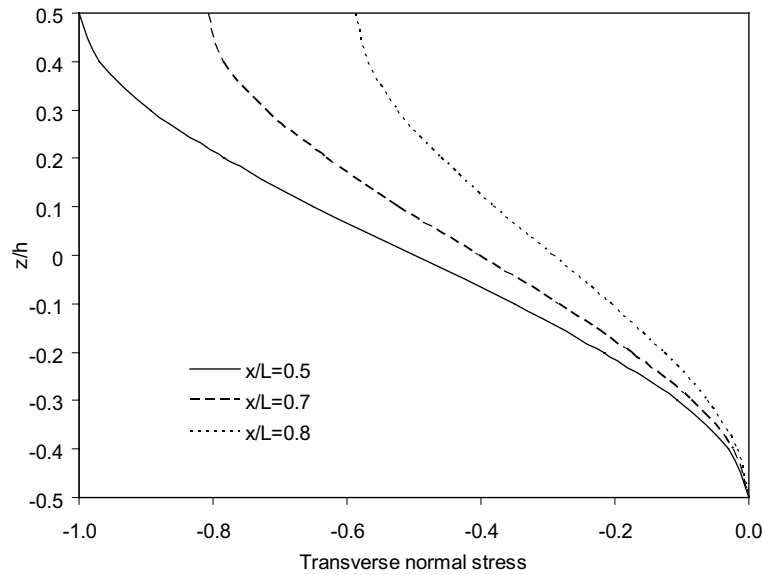


Fig. 4. Normalized transverse normal stress distribution, $\bar{\sigma}_z$, in a CF beam (corrector phase).

shear stress predictions onto the maximum shear stress corrector phase prediction, the point ($x = 0.25L$, $z = 0.2h$), which is allocated at the interface, is selected. Table 3 shows that regardless of the varying angles, span and stiffness ratios the correction percentage of the shear stress at the point ($0.25L, 0$) is always less than 3%. In more detail, when one keeps $L/h = 10$, $E_L/E_T = 25$, and changes α , the correction percentage of

Table 3

Normalised transverse shear parameters, $\bar{\tau}_{xz}(0.25L, z)$, of three-layered CC beam

α	L/h	E_L/E_T	Predictor	Corrector	Predictor	Predictor	Corrector
			$z = 0$	$z = 0$	$z = 0.2h + 0^+$	$z = 0.2h + 0^-$	$z = 0.2h$
15°	10	25	-0.3349	-0.3370	-0.2780	-0.2793	-0.2760
30°			-0.3434	-0.3497	-0.2677	-0.2779	-0.2635
45°			-0.3464	-0.3523	-0.2639	-0.2809	-0.2640
60°			-0.3421	-0.3437	-0.2723	-0.2839	-0.2756
75°			-0.3372	-0.3372	-0.2829	-0.2834	-0.2831
30°	4	25	-0.3451	-0.3536	-0.2175	-0.2516	-0.1994
	8		-0.3462	-0.3565	-0.2590	-0.2760	-0.2519
	15		-0.3397	-0.3414	-0.2773	-0.2800	-0.2767
	25		-0.3381	-0.3382	-0.2817	-0.2819	-0.2817
	50		-0.3377	-0.3377	-0.2831	-0.2831	-0.2831
30°	10	5	-0.3376	-0.3378	-0.2813	-0.2825	-0.2814
	10		-0.3389	-0.3403	-0.2778	-0.2812	-0.2773
	20		-0.3419	-0.3465	-0.2710	-0.2790	-0.2682
	30		-0.3447	-0.3528	-0.2646	-0.2769	-0.2590
	40		-0.3472	-0.3583	-0.2587	-0.2748	-0.2502

the shear stress is always less than 2%. At $\alpha = 75^\circ$, the shear stress values obtained through the predictor and corrector phases are practically identical. At $\alpha = 30^\circ$, $E_L/E_T = 25$ and $L/h = 8$, the correction percentage becomes as high as about 2.5%, but when the beam gets thinner, the agreement of shear stress values obtained through the predictor and corrector phases gets better. When $L/h > 15$, the shear stress predictions of the predictor and corrector phases are practically identical. At $L/h = 10$, $\alpha = 30^\circ$ and $E_L/E_T = 40$, the correction percentage is about 3%, but the agreement of shear stress predictor and corrector phases is improving with decreasing the stiffness ratio. Similar observations can be obtained at the point $(x = 0.25L, z = 0.2h)$, which is located at the interface of the same cross-section. It should be noted however that the observed discrepancies between the predictor and corrector phase shear stress predictions are still within the range of the engineering acceptable error (5%).

Table 3 shows however that the corrected shear stress value obtained at the material interface is not always between the two values originally predicted at the bottom of the upper layer and the top of lower layer. Fixing the span ratio at 10, the stiffness ratio at 25 and changing the material fibre aligning orientation, the correction percentage at the interface is always kept lower than 6%. The thinner the beam, the better the agreement of the shear stress predictor and corrector phases at the material interface. For $L/h > 15$ ($\alpha = 30^\circ$, $E_L/E_T = 25$), the shear stress predictor and corrector phases yield practically identical interlaminar shear stress values. The smaller the stiffness ratio, the better the agreement of the predictor and corrector phase shear stress values at the material interface. The results however show that the good agreement of maximum shear stresses obtained through the predictor and corrector phases at $z = 0$ is not significantly affected by the correction achieved in the interface shear stress values. For instance, when $\alpha = 30^\circ$, $E_L/E_T = 25$ and $L/h = 4$, the correction percentage of average shear stress value at the material interface $z = 0.2h$ is as large as about 15%, but at $z = 0$ the maximum shear stress correction is only about 2.5%. Such a low aspect ratio ($L/h = 4$) is however never used when stress analysis is performed on the basis of a shear deformable beam theory.

In a similar manner, Table 4 presents the variation of shear stress values for varying angles, span and stiffness ratios of a CF beam. This shows that regardless of the varying angles, span and stiffness ratios, the correction percentage of the shear stress at the point $(0.75L, 0)$ is always less than 4%. In more detail, when one keeps $L/h = 10$, $E_L/E_T = 25$ and changes α , the correction percentage of the shear stress is always less than 3%. At $L/h = 10$, $\alpha = 30^\circ$ and $E_L/E_T = 40$, the correction percentage is about 4%, but the agreement

Table 4

Normalised transverse shear parameters, $\bar{\tau}_{xz}(0.75L, z)$, of three-layered CF beam

α	L/h	E_L/E_T	Predictor	Corrector	Predictor	Predictor	Corrector
			$z = 0$	$z = 0$	$z = 0.2h + 0^+$	$z = 0.2h + 0^-$	$z = 0.2h$
15°	10	25	-0.1406	-0.1431	-0.1189	-0.1168	-0.1225
30°			-0.1407	-0.1375	-0.1225	-0.1106	-0.1278
45°			-0.1396	-0.1354	-0.1272	-0.1077	-0.1270
60°			-0.1385	-0.1380	-0.1261	-0.1112	-0.1215
75°			-0.1396	-0.1404	-0.1184	-0.1170	-0.1179
30°	4	25	-0.1454	-0.1461	-0.1288	-0.0850	-0.1536
	8		-0.1411	-0.1369	-0.1245	-0.1069	-0.1327
	15		-0.1402	-0.1386	-0.1199	-0.1144	-0.1223
	25		-0.1400	-0.1394	-0.1184	-0.1163	-0.1193
	50		-0.1399	-0.1397	-0.1177	-0.1172	-0.1179
30°	10	5	-0.1396	-0.1402	-0.1195	-0.1162	-0.1190
	10		-0.1398	-0.1395	-0.1207	-0.1146	-0.1213
	20		-0.1404	-0.1381	-0.1220	-0.1119	-0.1257
	30		-0.1410	-0.1369	-0.1229	-0.1093	-0.1299
	40		-0.1416	-0.1359	-0.1235	-0.1068	-0.1337

of shear stress predictor and corrector phases is again improving with decreasing the stiffness ratio. The observed discrepancies between the predictor and corrector phase maximum shear stress predictions are again within the range of the engineering acceptable error. Fixing however the span ratio at 10, the stiffness ratio at 25 but changing the material fibre aligning orientation, the correction percentage at the interface may become as big as 15%, which is about double the corresponding correction observed in the CC beam case. Agreement of the shear stress predictor and corrector phases at the material interface is however again improving when decreasing the beam thickness. For $L/h > 25$ ($\alpha = 30^\circ$, $E_L/E_T = 25$), the shear stress predictor and corrector phases yield again practically identical interlaminar shear stress values. The results however show again that the good agreement of maximum shear stresses obtained through the predictor and corrector phases at $z = 0$ is not significantly affected by the correction achieved in the interface shear stress values. For instance, when $\alpha = 30^\circ$, $E_L/E_T = 25$ and $L/h = 4$, the correction percentage of average shear stress value at the material interface $z = 0.2h$ is as large as about 44%, but at $z = 0$ the maximum shear stress correction is only about 0.5%. As is however already mentioned, stress analyses that are based on a shear deformable beam theory are reliable only for considerably large ratios ($L/h > 10$), for which the present approach appears to be undoubtedly successful.

3. Closure

It has been observed that, as far as SS angle-ply laminated beams are concerned, transverse shear stress distributions obtained through the predictor phase of G5DOFT are always practically identical with their corrector phase counterparts. Hence, the fact that transverse normal stress distributions cannot be obtained via the predictor phase of G5DOFT cannot anymore justify the use of the employed predictor–corrector method in connection with SS beams, for which the plane strain elasticity solution is available and can be easily reproduced from (Pagano, 1970). As far as other boundary conditions are concerned, the predictor–corrector approach can offer considerable improvement in the transverse shear stress distributions obtained through G5DOFT. Although that improvement appears to be below 5% for the maximum shear stress values it may considerably exceed that engineering acceptable error value for the interlaminar stresses.

It is therefore concluded that elasticity solutions for SS laminates cannot anymore be considered as safe means in checking and testing the effectiveness of conventional shear deformable theories (at least as far as angle-ply laminates are concerned (Pagano, 1970)). With the influence of end boundary conditions coming thus into the picture, some smaller or bigger relevant inaccuracies that the G5DOFT faces when dealing with clamped or free end boundaries are expected to considerably decrease by incorporating into the analysis the effects of transverse normal deformation (Soldatos and Watson, 1997a,b).

References

DiSciava, M., 1986. Bending, vibration and buckling of simply supported thick multilayered orthotropic plates: an evaluation of a new displacement model. *Journal of Sound and Vibration* 105, 425–442.

Heuer, R., 1992. Static and dynamic analysis of transversely isotropic, moderately thick sandwich beams by analogy. *Acta Mechanica* 91, 1–9.

Jane, K.C., Hong, C.C., 2000. Interlaminar stresses of a rectangular laminated plate with simply supported edges subject to free vibration. *International Journal of Mechanical Sciences* 42, 2031–2039.

Jones, R.M., 1975. *Mechanics of Composite Materials*. Hemisphere Publishing Corporation, New York.

Liu, S.L., 2001. Stress Analysis in Laminated Composites. PhD Thesis, Theoretical Mechanics Division, University of Nottingham.

Liu, S.L., Soldatos, K.P., 2002. On the prediction improvement of transverse stress distributions in cross-ply laminated beams: Advanced versus conventional beam modelling. *International Journal of Mechanical Sciences* 44, 287–304.

Noor, A.K., Burton, W.S., 1990. Predictor–corrector procedures for stress and free vibration analyses of multilayered composite plates and shells. *Computer Methods in Applied Mechanics and Engineering* 82, 341–363.

Noor, A.K., Malik, M., 1999. Accurate determination of transverse normal stresses in sandwich panels subjected to thermomechanical loadings. *Computer Methods in Applied Mechanics and Engineering* 178, 431–443.

Pagano, N.J., 1970. Influence of shear coupling in cylindrical bending of anisotropic laminates. *Journal of Composite Materials* 4, 330–343.

Reddy, J.N., 1984. A simple higher-order theory for laminated composite plates. *Journal of Applied Mechanics* 51, 745–752.

Ren, J.G., 1986. Bending theory of laminated plate. *Composites Science and Technology* 27, 225–248.

Savithri, S., Varadan, T.K., 1990. Free vibration and stability of cross-ply laminated plates. *Journal of Sound and Vibration* 141, 516–520.

Shu, X., Soldatos, K.P., 2000. Cylindrical bending of angle-ply laminates subjected to different sets of edge boundary conditions. *International Journal of Solids and Structures* 37, 4289–4307.

Soldatos, K.P., Liu, S.L., 2001. On the generalised plane strain deformations of thick anisotropic composite laminated plates. *International Journal of Solids and Structures* 38, 479–482.

Soldatos, K.P., Watson, P., 1997a. Accurate stress analysis of laminated plates combining a two-dimensional theory with the exact three-dimensional solution for simply supported edges. *Mathematics and Mechanics of Solids* 2, 459–489.

Soldatos, K.P., Watson, P., 1997b. A general theory for the accurate stress analysis of homogeneous and laminated composite beams. *International Journal of Solids and Structures* 22, 2857–2885.

Soldatos, K.P., Watson, P., 1997c. A method for improving the stress analysis performance of one- and two-dimensional theories for laminated composites. *Acta Mechanica* 123, 163–186.

Sun, C.T., Whitney, J.M., Whitford, L., 1975. Dynamic response of laminated composite plates. *American Institute of Aeronautics and Astronautics Journal* 13, 1259–1260.

Vel, S.S., Batra, R.C., 2000. The generalized plane strain deformations of thick anisotropic composite laminated plates. *International Journal of Solids and Structures* 37, 715–733.